CYBERNETICS AND PHYSICS, VOL. 13, NO. 2, 2024, 142–151

SYNCHRONIZATION OF COUPLED QUADCOPTERS USING CONTRACTION THEORY

Arpit Sharma
Department of Electrical Engineering
National Institute of Technology Kurukshetra
India
arpit860sharma@gmail.com

Jagdeep Singh Lather
Department of Electrical Engineering
National Institute of Technology Kurukshetra
India
jslather@nitkkr.ac.in

Article history:
Received 27.06.2024, Accepted 16.09.2024

Abstract

In this paper, the synchronization of coupled quadcopters using contraction theory principles is presented. In order to synchronize the roll and pitch angles of the quadcopter models, contraction theory application is a pivotal tool. Despite the fact that all of the quadcopters used in this study have identical characteristics, their behaviour greatly depends on their initial conditions. Because of the inherently nonlinear nature of quadcopters, slight variations in the initial conditions can have a significant impact on the trajectory of the quadcopters in the future. Contraction theory is a useful technique for addressing this problem. By using the contraction theory, synchronization has been done for two quadcopters as well as for three quadcopters. Finally, a generalized method for synchronizing any number of quadcopters using contraction theory is presented. For the synchronization of two quadcopters, roll angles and pitch angles were synchronized in 3.2 and 3.6 seconds, respectively whereas for the synchronization of three quadcopters, roll angles and pitch angles were synchronized in 3.2 and 3.4 seconds, respectively. MATLAB® is used to carry out the mathematical modelling of the quadcopters and the synchronization procedure.

Key words

Quadcopter, synchronization, contraction theory, modelling and nonlinear system.

1 Introduction

Quadcopters have become a vital part of modern society because of their many applications, which include delivery services, photography, agricultural activities, environmental monitoring, military use, and rescue missions [Ahmed et al., 2022]. However, effective quadcopter control requires advanced controllers capable of managing system non-linearity and maintaining a steady trajectory in any condition. Consequently, researchers have proposed linear and nonlinear, both kind of controllers to address such issues [Kadhim and Abdulsadda, 2022], [Kumar and Dewan, 2020]. The most popular choice for linear controllers is Proportional-Integral-Derivative and Linear Quadratic Regulator to efficiently govern quadcopter flight [Ahmad et al., 2020], [Saini and Ohri, 2023]. These controllers are very simple to design and execute, but in noisy and uncertain environments, they are unable to deliver the desired outcomes. Researchers have developed different nonlinear controllers to tackle this issue, including reinforcement learning based controllers [Barzegar and Lee, 2022], model predictive controllers [Ribeiro et al., 2015], sliding mode controllers [Yagiz et al., 2011], [Kumar and Dewan, 2023b], [Kumar and Dewan, 2023a] and feedback linearization controllers [Lee et al., 2009], [Rigatos, 2021] to improve performance, especially in noisy or disturbed environments. The deployment of a coordinated squadron of quadcopters instead of a single vehicle is significantly more effective in many mission circumstances. This is especially apparent in applications like tracking, mapping, and swarm robots [Blais and Akhloufi, 2023]. Managing and coordinating a swarm of quadcopters is a difficult task that requires synchronization, formation, flocking, consensus, and rendezvous procedures that are customised to meet particular needs [Enwerem and Baras, 2023a]. In [Enwerem and Baras, 2023b], the authors proposed control strategies that use both centralised and decentralised approaches to enable the coordinated functioning of several quadcopter units. Quadcopter synchronization depends on communication network reliability, and a lot of study looks at communication protocol effects [Sharma et al., 2020]. In [Yanmaz et al., 2018], Different communication ranges have been taken into consideration while

discussing the synchronization of quadcopter networks, which is particularly helpful in situations where there are quadcopters with varied capabilities or sensor ranges. Furthermore, researchers also investigate how sensor fusion methods can improve the synchronization process [Zhang et al., 2023]. Human engagement is sometimes required for the efficient synchronization and control of quadcopter swarms. This emphasises how important it is to have user-friendly control interfaces that provide an acceptable method for people to interact with swarms of quadcopters [Bjurling et al., 2020]. Quadcopter synchronization is complicated by its nonlinear dynamics of quadcopters. Researchers deal with the complexities of quadcopter modelling and control, attempting to reduce problems like trajectory variations due to the initial conditions and external disturbances [Hehn and D'Andrea, 2011]. Moreover, it is still crucial to guarantee the safety and reliability of synchronized quadcopters, with fault tolerance and redundancy identified as essential components to guarantee the secure and reliable coordination between multiple quadcopters [Nguyen et al., 2023].

This work primarily deals with contraction theory to effectively synchronize the roll and pitch angles of coupled quadcopters. Contraction theory, which is generally used for the synchronization of chaotic systems, is employed in the context of quadcopters, where it is use to synchronize the trajectories of two quadcopters and three quadcopters and then a generalised method is proposed to synchronize any number of quadcopters. The structure of this paper is as follows: in section 1, quadcopters are introduced and the importance of synchronization is highlighted. A complete quadcopter mathematical model is provided in section 2. The introduction of contraction theory and its application in the synchronization process is examined in section 3. The simulations and results are presented in section 4, which demonstrate the synchronization methodology's implementations and outcomes. section 5 concludes with a summary of the main conclusions.

2 Quadcopter Model

A quadcopter is an underactuated system because it has more outputs than inputs. The total degree of freedom of the quadcopter is six, which is achieved by the different speed combinations of propellers. These combinations decide the trajectory of the quadcopter. The quadcopter motion is defined by two different coordinate frames in space: one is a body-fixed frame, $B = [x_B, y_B, z_B]$, and the other is an earth-fixed frame or inertial-fixed frame, $G = [X, Y, Z]$ as shown in Figure 1 [Ivanov et al., 2024]. In a quadcopter, there are broadly two types of parameters: one is rotational parameters, and the other is translational parameters.

The coordinates x (East), y (North), and z (Up) are used to describe the quadcopter's position with respect to the inertial reference frame, which is a fixed point on the globe. The rotating angles are represented by ϕ, θ, and $\psi \in \mathbb{R}$, where:

$$-\frac{\pi}{2} \leq \phi \leq \frac{\pi}{2}, \quad -\frac{\pi}{2} \leq \theta \leq \frac{\pi}{2}, \quad -\pi \leq \psi \leq \pi$$

where ϕ represents the roll angle, θ represents the pitch angle, and ψ represents the yaw angle. ϕ, θ, and ψ are also known as the Euler angles, and $\dot{\phi}$, $\dot{\theta}$, and $\dot{\psi}$ are known as the Euler angle velocities.

Angular velocities with respect to the inertial frame G can be converted to angular velocities with respect to the body-fixed frame B using the transformation matrix T [Chovancová et al., 2014].

$$T = \begin{bmatrix} 1 & 0 & -\sin\theta \\ 0 & \cos\phi & \cos\theta\sin\phi \\ 0 & -\sin\phi & \cos\theta\cos\phi \end{bmatrix}$$

The reverse transformation of angular velocities can be obtained by the inverse of the transformation matrix T^{-1}.

$$T^{-1} = \begin{bmatrix} 1 & \sin\phi\tan\theta & \cos\phi\tan\theta \\ 0 & \cos\phi & -\sin\phi \\ 0 & \frac{\sin\phi}{\cos\theta} & \frac{\cos\phi}{\cos\theta} \end{bmatrix}$$

For quadcopter small angle assumption has been taken as $\phi \approx \theta \approx 0$. by which T and T^{-1} become identity matrix. The other assumptions taken in this paper are following [Ivanov et al., 2024]:

1) There is rigidity and symmetry in the quadcopter's architecture around the vertical axis.

2) The body-fixed frame origin and center of gravity coincide

3) The structure's bending can be neglected.

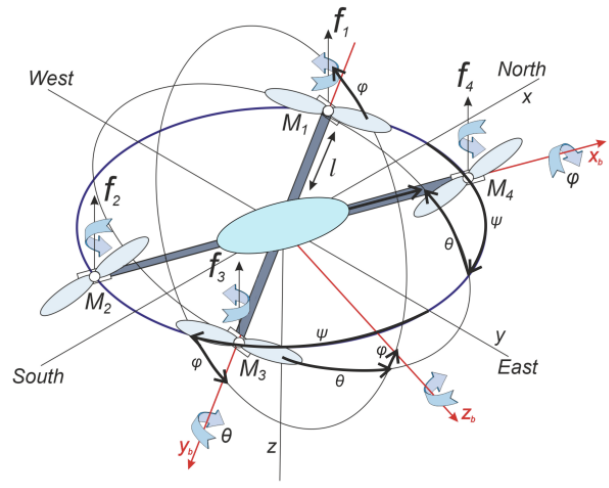

Figure 1. Quadcopter Model

The following is the complete dynamic model (rotational and translational) that controls the quadcopter

[Thanh and Hong, 2018]:

$$\begin{cases} \ddot{\phi} = \frac{(J_y - J_z)}{J_x}\dot{\theta}\dot{\psi} + \frac{l}{J_x}u_2 + \dot{\theta}\frac{J_r}{J_x}\tau_r \\ \ddot{\theta} = \frac{(J_z - J_x)}{J_y}\dot{\phi}\dot{\psi} + \frac{l}{J_y}u_3 - \dot{\phi}\frac{J_r}{J_y}\tau_r \\ \dot{\psi} = \frac{(J_x - J_y)}{J_z}\dot{\theta}\dot{\phi} + \frac{1}{J_z}u_4 \\ \ddot{z} = \frac{u_1}{m}(c\phi c\theta c\phi) - g \\ \ddot{x} = \frac{u_1}{m}(c\phi s\theta c\psi + s\phi s\psi) \\ \ddot{y} = \frac{u_1}{m}(c\phi s\theta c\psi - s\phi s\psi) \end{cases} \tag{1}$$

The dynamic mathematical quadcopter model includes J_x (about x-axis), J_y (about y -axis) and J_z (about z -axis), which are inertias, whereas J_r represents the inertia of the motor and τ_r represents the residual angular velocity of the rotor. the definitions of these and other parameters as well as their values [Thanh and Hong, 2018]. For simplification, the state space model has been achieved with the help of the dynamic model of the quadcopter.

$$\dot{Z} = f(Z, u) \tag{2}$$

where Z represents the state vector and u represents the input vector,

$$\begin{cases} Z = |Z_1, Z_2, Z_3, Z_4, Z_5, Z_6, Z_7, Z_8, Z_9, Z_{10}, Z_{11}, Z_{12}| \\ Z = |\phi, \dot{\phi}, \theta, \dot{\theta}, \dot{\psi}, \dot{\psi}, z, \dot{z}, x, \dot{x}, y, \dot{y}| \end{cases}$$

and,

$$u = |u_1, u_2, u_3, u_4|$$

Then,

$$\dot{Z} = \begin{cases} \dot{Z}_1 = Z_2 \\ \dot{Z}_2 = a_1 Z_4 Z_6 + a_2 Z_4 \tau_r + b_1 u_2 \\ \dot{Z}_3 = Z_4 \\ \dot{Z}_4 = a_3 Z_2 Z_6 + a_4 Z_2 \tau_r + b_2 u_3 \\ \dot{Z}_5 = Z_6 \\ \dot{Z}_6 = a_5 Z_2 Z_4 + b_3 u_4 \\ \dot{Z}_7 = Z_8 \\ \dot{Z}_8 = \frac{1}{m}(cZ_1 cZ_3)\, u_1 - g \\ \dot{Z}_9 = Z_{10} \\ \dot{Z}_{10} = \frac{1}{m}(u_x u_1) \\ \dot{Z}_{11} = Z_{12} \\ \dot{Z}_{12} = \frac{1}{m}(u_y u_1) \end{cases} \tag{3}$$

where,

$$\begin{cases} a_1 = \frac{(J_y - J_z)}{J_x}, a_3 = \frac{(J_z - J_x)}{J_y} \\ a_5 = \frac{(J_x - J_y)}{J_z}, a_2 = \frac{J_r}{J_x}, a_4 = -\frac{J_r}{J_y} \\ b_1 = \frac{l}{J_x}, b_2 = \frac{l}{J_y}, b_3 = \frac{1}{J_z} \end{cases}$$

In a quadcopter, the forces and torques are used as control inputs and are controlled by adjusting the motor speeds. The lift force generated by each motor is proportional to the square of its speed, while torques for roll, pitch, and yaw are produced by differential thrust between the motors. The control system computes the required forces and torques and converts them into corresponding motor speed adjustments to achieve the desired movement.

$$\begin{cases} u_1 = b\left(\omega_1^2 + \omega_2^2 + \omega_3^2 + \omega_4^2\right) \\ u_2 = b\left(-\omega_2^2 + \omega_4^2\right) \\ u_3 = b\left(-\omega_1^2 + \omega_3^2\right) \\ u_4 = d\left(-\omega_1^2 + \omega_2^2 - \omega_3^2 + \omega_4^2\right) \end{cases} \tag{4}$$

u_1, u_2, u_3 and u_4 are the control inputs. Here b stands for the lift coefficient, d stands for drag coefficient and $omega_i = (i = 1, 2, 3, 4)$ represents propeller speeds.

3 Contraction Theory

Contraction is a property regarding the convergence of two system trajectories. If initial conditions or temporary disruptions of a nonlinear time-varying dynamic system are shrunk exponentially fast, it must be said that the system will be contracting, i.e., the trajectory of the perturbed system converges exponentially to its nominal behavior [Sharma and Handa, 2022]. Two quadcopters are shown in Figure 2 which are bi-directionally coupled to each other, they have different responses due to the different initial conditions but after the application of contraction theory, their responses are synchronized to a single trajectory. Consider a nonlinear system:

$$\dot{z} = f(z, t) \tag{5}$$

where f is an $m \times 1$ vector function and $\mathbf{z} \in \mathbb{R}^m$ is the state vector. Assuming $f(\mathbf{z}, t)$ is continuously differentiable, then we have [Yao and Liu, 2010]:

$$\frac{d(\delta z^T \delta z)}{dt} = 2\delta z^T \dot{\delta z} = 2\delta z^T \frac{\partial f}{\partial z}\delta z \leq 2\lambda_{\max}\delta z^T \delta z \tag{6}$$

and,

$$\|\delta z\| \leq \|\delta z_0\| e^{\int_0^t \lambda_{\max}(z,t)\, dt} \tag{7}$$

where $\lambda_{\max}$ is the largest eigenvalue of the symmetric component of the Jacobian $J = \frac{\partial f}{\partial z}$, and δz stands for the virtual distance between two trajectories. For the convergence of any infinitesimal length $\|\delta z\|$ exponentially to zero, $\lambda_{\max}$ must be uniformly negative definite [Yao and Liu, 2010].

For the system to be synchronized, the condition is that the symmetric part of the Jacobian matrix must be negative definite. In this work, two quadcopter systems have been considered, which are supposed to be synchronized. For this, a virtual system has been created that represents both systems. Both systems are coupled (bi-directional) as shown in Figure 3.

Here, Z_2 and Z_{14} are the two trajectories of different systems, and k_1 is the coupling strength, which indicates

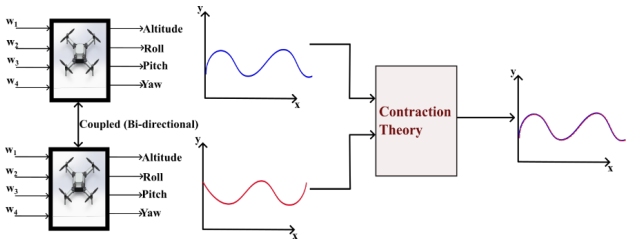

Figure 2. Structure of contraction theory for two quadcopters

how tightly the systems are coupled to each other. The coupling part is represented by $k_1(Z_{14} - Z_2)$ for Figure 3(a), which is a forward coupling, and $k_1(Z_2 - Z_{14})$ for Figure 3(b), which is a backward coupling. Alternatively, these couplings can be represented by Figure 3(c), which shows a bi-directional coupling.

This presentation is shown for roll angles, but it can similarly be applied to pitch and yaw angles.

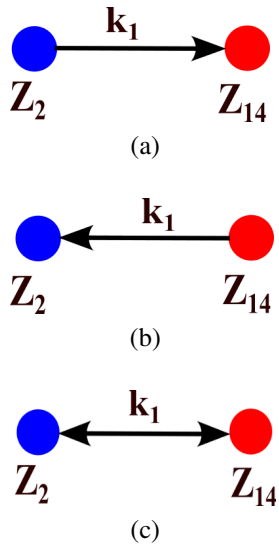

Figure 3. Coupling of two nonlinear systems: (a) Forward coupling, (b) Backward coupling, (c) Bi-directional coupling

Corollary: Suppose two n-dimensional nonlinear systems:

$$\dot{A} = F(A) + H(B) - H(A) \tag{8}$$

$$\dot{B} = F(B) + H(A) - H(B) \tag{9}$$

The virtual system of the above equations can be built as:

$$\gamma(C, A, B) = F(C) - 2H(C) + H(A) + H(B) \tag{10}$$

This virtual system represents both systems (equation (8) and equation (9)), as $\dot{A} = \gamma(A, A, B)$ and $\dot{B} = \gamma(B, A, B)$.

The connected systems will be synchronized if the virtual system is contracting with respect to the virtual γ-variable [Sharma and Handa, 2022].

3.1 Contraction Theory Application for Two Quadcopters

For this work, two identical quadcopters have been taken. The initial conditions are different for both quadcopters. Due to the highly nonlinear system, the future trajectories will be different. In this work, synchronization has been done for roll and pitch angles so we can consider the rotational part only.

Let the rotational part of the first system be represented as;

$$\begin{cases} \dot{Z}_2 = a_1 Z_4 Z_6 + a_2 Z_4 \tau_r + b_1 u_2 \\ \dot{Z}_4 = a_3 Z_2 Z_6 + a_4 Z_2 \tau_r + b_2 u_3 \\ \dot{Z}_6 = a_5 Z_2 Z_4 + b_3 u_4 \end{cases} \tag{11}$$

Where Z_2, Z_4, and Z_6 represent the roll, pitch, and yaw angles of the first quadcopter and are denoted by ϕ_1, θ_1, and ψ_1, respectively.

And rotational part of other systems is represented as;

$$\begin{cases} \dot{Z}_{14} = a_1 Z_{16} Z_{18} + a_2 Z_{16} \tau_r + b_1 u_2 \\ \dot{Z}_{16} = a_3 Z_{14} Z_{18} + a_4 Z_{14} \tau_r + b_2 u_3 \\ \dot{Z}_{18} = a_5 Z_{14} Z_{16} + b_3 u_4 \end{cases} \tag{12}$$

Where Z_{14}, Z_{16}, and Z_{18} represent the roll, pitch, and yaw angles of the second quadcopter and are denoted by ϕ_2, θ_2, and ψ_2, respectively.Consider that both systems are coupled with a coupling strength of k_i (for $i = 1, 2, 3$).

The system 11 and 12 become;

$$\begin{cases} \dot{Z}_2 = a_1 Z_4 Z_6 + a_2 Z_4 \tau_r + b_1 u_2 + k_1(Z_{14} - Z_2) \\ \dot{Z}_4 = a_3 Z_2 Z_6 + a_4 Z_2 \tau_r + b_2 u_3 + k_2(Z_{16} - Z_4) \\ \dot{Z}_6 = a_5 Z_2 Z_4 + b_3 u_4 + k_3(Z_{18} - Z_6) \end{cases} \tag{13}$$

and

$$\begin{cases} \dot{Z}_{14} = a_1 Z_{16} Z_{18} + a_2 Z_{16} \tau_r + b_1 u_2 + k_1(Z_2 - Z_{14}) \\ \dot{Z}_{16} = a_3 Z_{14} Z_{18} + a_4 Z_{14} \tau_r + b_2 u_3 + k_2(Z_4 - Z_{16}) \\ \dot{Z}_{18} = a_5 Z_{14} Z_{16} + b_3 u_4 + k_3(Z_6 - Z_{18}) \end{cases} \tag{14}$$

With the help of systems 13 and 14 virtual system can be constructed like;

$$\begin{cases} \dot{p} = a_1 qr + a_2 q\tau_r + b_1 u_2 - 2k_1 p + k_1(Z_2 + Z_{14}) \\ \dot{q} = a_3 pr + a_4 p\tau_r + b_2 u_3 - 2k_2 q + k_2(Z_4 + Z_{16}) \\ \dot{r} = a_5 pq + b_3 u_4 - 2k_3 r + k_3(Z_6 + Z_{18}) \end{cases} \tag{15}$$

System 15 represents both systems (13 and 14). After substituting $p = Z_2$, $q = Z_4$, and $r = Z_6$, system 13 is obtained. Similarly, after substituting $p = Z_{14}$, $q = Z_{16}$, and $r = Z_{18}$, system 14 is obtained.

For the synchronization of systems 13 and 14, the symmetric part of the Jacobian of the virtual system should be negative definite.

Let system 15 be:

$$\dot{N} = \xi(N), \quad \text{where} \quad N = (p, q, r) \in \mathbb{R}^3.$$

The Jacobian Λ of system 17 is:

$$\Lambda = \frac{\partial \xi}{\partial N} = \begin{bmatrix} -2k_1 & a_1 r + a_2 \tau_r & a_1 q \\ a_3 r + a_4 \tau_r & -2k_2 & a_3 p \\ a_5 q & a_5 p & -2k_3 \end{bmatrix}$$

The symmetric part $\mathcal{A}$ of the Jacobian is calculated as:

$$\mathcal{A} = \frac{1}{2}(\Lambda + \Lambda^T)$$

After substituting the parameter values, the symmetric part $\mathcal{A}$ of the Jacobian becomes:

$$\mathcal{A} = \begin{bmatrix} -2k_1 & 0 & -\frac{q}{2} \\ 0 & -2k_2 & \frac{p}{2} \\ -\frac{q}{2} & \frac{p}{2} & -2k_3 \end{bmatrix}$$

The conditions for the matrix to be negative definite are:

$$\begin{cases} k_1 > 0, \\ k_2 > 0, \\ k_3 > 0. \end{cases}$$

The contraction region is defined as:

$$C : \left\{ (p, q, r) : \frac{p^2}{16 k_2 k_3} + \frac{q^2}{16 k_1 k_3} < 1 \right\}$$

Thus, every solution that begins with any initial condition will stay in C and converge exponentially to a single path.

3.2 Contraction Theory Application for Three Quadcopters

For the synchronization of three quadcopters same strategy has been followed. A virtual system is formulated which represents all three systems. The first two systems are taken the same as in equations 11 and 12. The third system is considered as;

$$\begin{cases} \dot{Z}_{26} = a_1 Z_{28} Z_{30} + a_2 Z_{28} \tau_r + b_1 u_2 \\ \dot{Z}_{28} = a_3 Z_{26} Z_{30} + a_4 Z_{26} \tau_r + b_2 u_3 \\ \dot{Z}_{30} = a_5 Z_{26} Z_{28} + b_3 u_4 \end{cases} \tag{16}$$

Where Z_{26}, Z_{28}, and Z_{30} represent the roll, pitch, and yaw angles of the third quadcopter and are denoted by ϕ_3, θ_3, and ψ_3, respectively.

All three systems are coupled (bi-directional) as shown in Figure 4, where Z_2, Z_{14}, and Z_{26} are the trajectories of the different systems, and k_1 is the coupling strength, indicating how tightly the systems are coupled to each other. This presentation has been shown for roll angles; similarly, it can be achieved for pitch and yaw angles.

$$\begin{cases} \dot{Z}_2 = a_1 Z_4 Z_6 + a_2 Z_4 \tau_r + b_1 u_2 - 2k_1 Z_2 \\ \qquad +k_1 Z_{14} + k_1 Z_{26} \\ \dot{Z}_4 = a_3 Z_2 Z_6 + a_4 Z_2 \tau_r + b_2 u_3 - 2k_2 Z_4 \\ \qquad +k_2 Z_{16} + k_2 Z_{28} \\ \dot{Z}_6 = a_5 Z_2 Z_4 + b_3 u_4 - 2k_3 Z_6 \\ \qquad +k_3 Z_{18} + k_3 Z_{30} \end{cases} \tag{17}$$

$$\begin{cases} \dot{Z}_{14} = a_1 Z_{16} Z_{18} + a_2 Z_{16} \tau_r + b_1 u_2 - 2k_1 Z_{14} \\ \qquad +k_1 Z_2 + k_1 Z_{26} \\ \dot{Z}_{16} = a_3 Z_{14} Z_{18} + a_4 Z_{14} \tau_r + b_2 u_3 - 2k_2 Z_{16} \\ \qquad +k_2 Z_4 + k_2 Z_{28} \\ \dot{Z}_{18} = a_5 Z_{14} Z_{16} + b_3 u_4 - 2k_3 Z_{18} \\ \qquad +k_3 Z_6 + k_3 Z_{30} \end{cases} \tag{18}$$

and,

$$\begin{cases} \dot{Z}_{26} = a_1 Z_{28} Z_{30} + a_2 Z_{28} \tau_r + b_1 u_2 - 2k_1 Z_{26} \\ \qquad +k_1 Z_2 + k_1 Z_{14} \\ \dot{Z}_{28} = a_3 Z_{26} Z_{30} + a_4 Z_{26} \tau_r + b_2 u_3 - 2k_2 Z_{28} \\ \qquad +k_2 Z_4 + k_2 Z_{16} \\ \dot{Z}_{30} = a_5 Z_{26} Z_{28} + b_3 u_4 - 2k_3 Z_{30} \\ \qquad +k_3 Z_6 + k_3 Z_{18} \end{cases} \tag{19}$$

With the help of systems 17, 18 and 19, a virtual system is formulated which looks like;

$$\begin{cases} \dot{p} = a_1 q r + a_2 q \tau_r + b_1 u_2 - 3k_1 p \\ \qquad +k_1 (Z_2 + Z_{14} + Z_{26}) \\ \dot{q} = a_3 p r + a_4 p \tau_r + b_2 u_3 - 3k_2 q \\ \qquad +k_2 (Z_4 + Z_{16} + Z_{28}) \\ \dot{r} = a_5 p q + b_3 u_4 - 3k_3 r \\ \qquad +k_3 (Z_6 + Z_{18} + Z_{30}) \end{cases} \tag{20}$$

Virtual System 20 represents all three systems (17, 18, and 19). After substituting $p = Z_2$, $q = Z_4$, and $r = Z_6$, system 17 is achieved. Similarly, after substituting $p = Z_{14}$, $q = Z_{16}$, and $r = Z_{18}$, system 18 is achieved, and for $p = Z_{26}$, $q = Z_{28}$, and $r = Z_{30}$, system 19 is achieved. For the synchronization of systems 17, 18, and 19, the symmetric part of the Jacobian of the virtual system should be negative definite.

Let system 20 be:

$$\dot{M} = \xi(M), \quad \text{where} \quad M = (p, q, r) \in \mathbb{R}^3.$$

The Jacobian of system 20 is:

$$B = \frac{\partial \xi}{\partial M} = \begin{bmatrix} -3k_1 & a_1 r + a_2 \tau_r & a_1 q \\ a_3 r + a_4 \tau_r & -3k_2 & a_3 p \\ a_5 q & a_5 p & -3k_3 \end{bmatrix}$$

$$\mathcal{A} = \begin{bmatrix} -2k_1 & \frac{1}{2}(a_1 r + a_2\tau_r + a_3 r + a_4\tau_r) & \frac{1}{2}(a_1 q + a_5 q) \\ \frac{1}{2}(a_1 r + a_2\tau_r + a_3 r + a_4\tau_r) & -2k_2 & \frac{1}{2}(a_3 p + a_5 p) \\ \frac{1}{2}(a_1 q + a_5 q) & \frac{1}{2}(a_3 p + a_5 p) & -2k_3 \end{bmatrix}$$

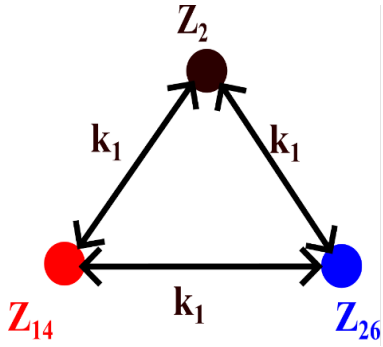

Figure 4. Bi-directional coupling of three nonlinear systems

The symmetric part of Jacobian is calculated as:

$$\mathcal{B} = \frac{1}{2}(B + B^T)$$

$$\mathcal{B} = \begin{bmatrix} -3k_1 & 0 & -\frac{q}{2} \\ 0 & -3k_2 & \frac{p}{2} \\ -\frac{q}{2} & \frac{p}{2} & -3k_3 \end{bmatrix}$$

Conditions for the negative definite matrix are:

$$\begin{cases} k_1 > 0 \\ k_2 > 0 \\ k_3 > 0 \end{cases}$$

And the contraction region is:

$$C : \left\{ (p, q, r) \mid \frac{p^2}{36k_2k_3} + \frac{q^2}{36k_1k_3} < 1 \right\}$$

3.3 Contraction Theory Application for n-Quadcopters

This section presents the general method for synchronization of n-quadcopters. The virtual system for the synchronization of n-quadcopters looks like;

$$\begin{cases} \dot{p} = a_1 qr + a_2 q\tau_r + b_1 u_2 - nk_1 p \\ \quad\quad +k_1 \sum_{i=0}^{n-1} Z_{2+12i} \\ \dot{q} = a_3 pr + a_4 p\tau_r + b_2 u_3 - nk_2 q \\ \quad\quad +k_2 \sum_{i=0}^{n-1} Z_{4+12i} \\ \dot{r} = a_5 pq + b_3 u_4 - nk_3 r \\ \quad\quad +k_3 \sum_{i=0}^{n-1} Z_{6+12i} \end{cases} \tag{21}$$

The corresponding Symmetric part of Jacobian is calculated as;

$$\mathcal{B} = \begin{bmatrix} -nk_1 & 0 & -\frac{q}{2} \\ 0 & -nk_2 & \frac{p}{2} \\ -\frac{q}{2} & \frac{p}{2} & -nk_3 \end{bmatrix}$$

And the contraction region is:

$$C : \left\{ (p, q, r) \mid \frac{p^2}{4n^2k_2k_3} + \frac{q^2}{4n^2k_1k_3} < 1 \right\}$$

4 Simulation and Results

MATLAB® has been used for the verification of this work. Two scenarios have been considered:

Scenario-I: Synchronization of two quadcopter models.
Scenario-II: Synchronization of three quadcopter models.

The condition for a quadcopter to start the altitude operation is that the force u_1 must be greater than the gravitational force, i.e., $u_1 > mg$. After using the parameter values, u_1 must be greater than 10.976 N. Additionally, $\omega_1, \omega_2, \omega_3, \omega_4$ are the same for the hover condition, which should be equal to 595.80 r/s.
For forward pitch operation, $\omega_3 = \omega_4 > \omega_1 = \omega_2$. Thus, the assumption is that the speed of the propellers are $\omega_1 = \omega_2 = 600$ r/s and $\omega_3 = \omega_4 = 605$ r/s. Similarly, for clockwise roll operation, $\omega_2 = \omega_3 > \omega_1 = \omega_4$. Thus, the assumption is that the speed of the propellers are $\omega_2 = \omega_3 = 605$ r/s and $\omega_1 = \omega_4 = 600$ r/s. In both operations, the yaw moment is zero, so it has not been considered.

4.1 Synchronization of Two Quadcopters

Synchronization has been done for the roll and pitch angles of two identical quadcopters. The design parameters are the same for both systems, but the difference is in the initial conditions. When initial conditions are zero, the roll angle and pitch angle trajectories follow the same path for both quadcopters, as shown in Figure 5. For the first system, the initial conditions are $\phi_{10}, \theta_{10}, \psi_{10} = (-3, -2, 0)$, and for the second system, the initial conditions are $\phi_{20}, \theta_{20}, \psi_{20} = (3, 2, 0)$. The initial condition for yaw is taken as zero because the yaw angle is not considered in this work. Figure 6 shows that without contraction theory, the systems do not follow the same trajectory even when the system parameters are the same for both systems. After applying the contraction theory, both systems start following the same trajectory, as seen in Figure 7. The coupling strength is

$$\mathcal{B} = \frac{1}{2}\begin{bmatrix} -3k_1 & \frac{1}{2}(a_1 r + a_2\tau_r + a_3 r + a_4\tau_r) & \frac{1}{2}(a_1 q + a_5 q) \\ \frac{1}{2}(a_1 r + a_2\tau_r + a_3 r + a_4\tau_r) & -3k_2 & \frac{1}{2}(a_3 p + a_5 p) \\ \frac{1}{2}(a_1 q + a_5 q) & \frac{1}{2}(a_3 p + a_5 p) & -3k_3 \end{bmatrix}$$

taken as $(k_1, k_2, k_3) = (1, 1, 1)$. The error between the trajectories after the application of contraction is shown in Figure 8. Specifications, which include synchronization time and steady-state error, are presented in Table 2 for a better understanding of performance.

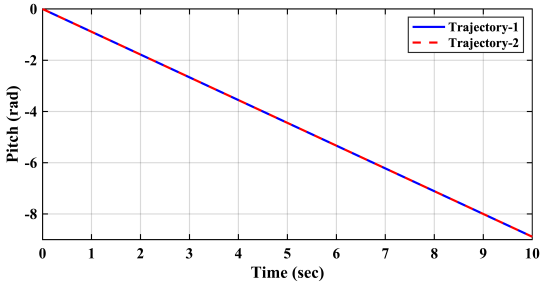

(a)

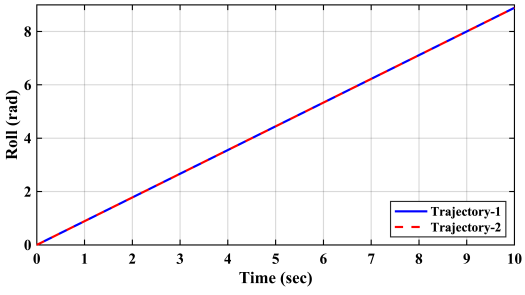

(b)

Figure 5. Synchronization (With zero initial conditions) for (a) Pitch, (b) Roll

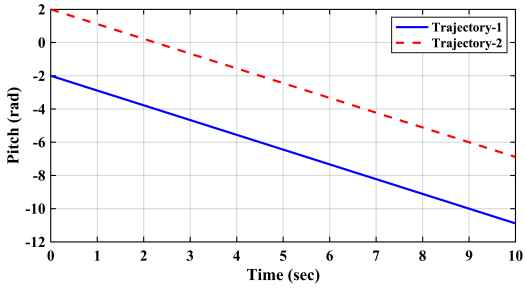

(a)

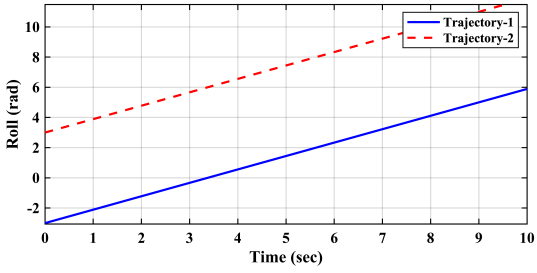

(b)

Figure 6. Synchronization (With different initial conditions) for (a) Pitch, (b) Roll

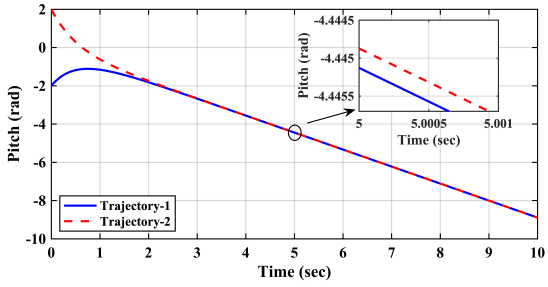

(a)

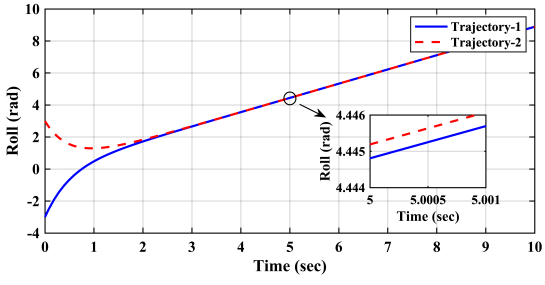

(b)

Figure 7. Synchronization (With different initial conditions after contraction theory) for (a) Pitch, (b) Roll

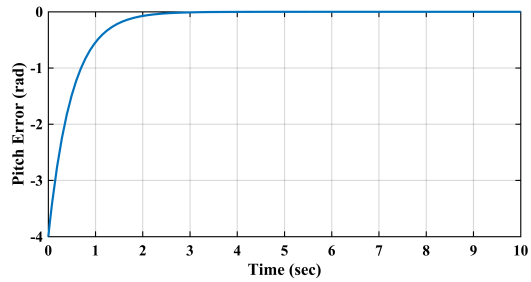

(a)

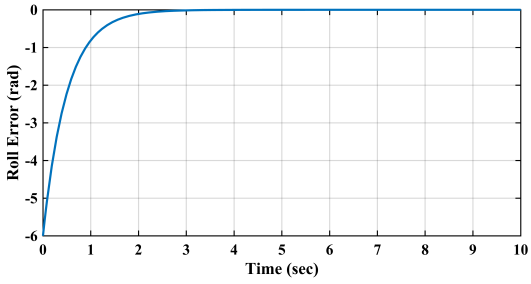

(b)

Figure 8. Synchronization error (With different initial conditions after contraction theory) for (a) Pitch, (b) Roll

4.2 Synchronization of Three Quadcopters

Like two systems synchronization, three systems synchronization has also been done in this paper. Initial conditions for system one is $\phi_{10}, \theta_{10}, \psi_{10} = (-2, -3, 0)$, for system two is $\phi_{20}, \theta_{20}, \psi_{20} = (2, 3, 0)$, and for system three is $\phi_{30}, \theta_{30}, \psi_{30} = (1, 1, 0)$. Before the contraction theory application, all the trajectories followed altogether different paths because of the different initial conditions but after the contraction theory application, all the trajectories followed the same path for both, roll angle and pitch angle which is shown in Figure 9. Coupling strength is taken as $(k_1, k_2, k_3) = (0.7, 0.7, 2)$. Errors between trajectories, after the application of contraction theory are shown in Figure 10. Table 3 presents performance specifications, encompassing synchronization time and steady-state error.

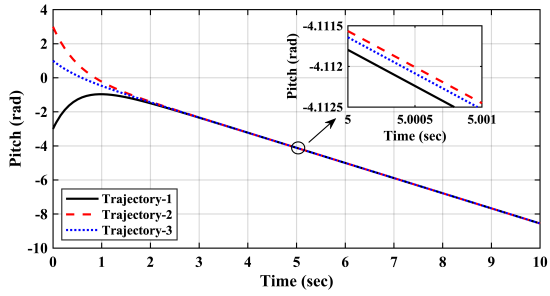

(a)

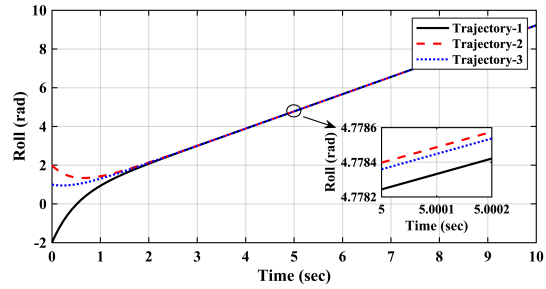

(b)

Figure 9. Synchronization (With different initial conditions after contraction theory) for (a) Pitch, (b) Roll

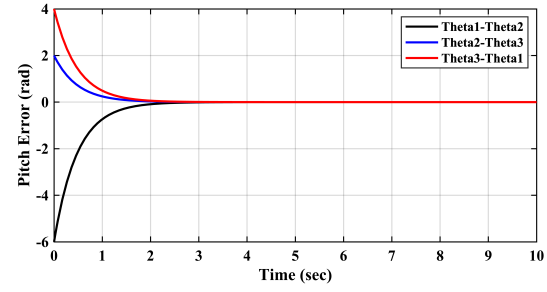

(a)

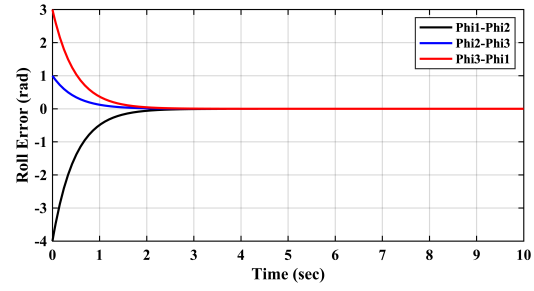

(b)

Figure 10. Synchronization error (With different initial conditions and contraction theory) for (a) Pitch, (b) Roll

5 Conclusions

This research employs the concept of contraction theory to achieve the synchronization of n-quadcopter models. The key finding of this work is that identical quadcopter models follow the same trajectories when initial conditions are the same, specifically with regard to roll and pitch angles. However, even a small change in the initial conditions of quadcopters has a significant effect on the scenario. In order to tackle this difficulty and

Table 1. Performance Specifications for two synchronized quadcopters

	Steady State Error before contraction theory application (rad)	Steady State Error after contraction theory application (rad)	Synchronization Time after the application of contraction theory (sec)
Pitch	4	0.00042	3.6
Roll	6	0.00023	3.2

Table 2. Performance Specifications for three synchronized quadcopters

	Steady State Error (Quadcopter 1 – Quadcopter 2)	Steady State Error (Quadcopter 2 – Quadcopter 3)	Steady State Error (Quadcopter 3 – Quadcopter 1)	Synchronization Time after the application of contraction theory (sec)
Pitch	0.00015	0.00006	0.00009	3.4
Roll	0.00012	0.00003	0.00009	3.2

enable effective and rapid synchronization of the systems, this work makes use of the contraction theory principle, which permits the quadcopters to continue moving in sync even when the initial conditions are different. First, this technique is applied on two quadcopters, which took 3.2 seconds and 3.6 seconds to achieve the synchronization of roll angles and pitch angles, respectively the same concept is applied to the synchronization of three quadcopters which took 3.2 seconds and 3.6 seconds for the synchronization of roll angles and pitch angles, respectively. By using these two scenarios, a generalized approach is proposed which is able to synchronize any number of quadcopters.

References

Ahmad, F., Kumar, P., Bhandari, A., and Patil, P. P. (2020). Simulation of the quadcopter dynamics with lqr based control. *Materials Today: Proceedings*, **24**, pp. 326–332.

Ahmed, F., Mohanta, J., Keshari, A., and Yadav, P. S. (2022). Recent advances in unmanned aerial vehicles: a review. *Arabian Journal for Science and Engineering*, **47** (7), pp. 7963–7984.

Barzegar, A. and Lee, D.-J. (2022). Deep reinforcement learning-based adaptive controller for trajectory tracking and altitude control of an aerial robot. *Applied Sciences*, **12** (9), pp. 4764.

Bjurling, O., Granlund, R., Alfredson, J., Arvola, M., and Ziemke, T. (2020). Drone swarms in forest firefighting: A local development case study of multi-level human-swarm interaction. In *Proceedings of the 11th Nordic Conference on Human-Computer Interaction: Shaping Experiences, Shaping Society*, pp. 1–7.

Blais, M.-A. and Akhloufi, M. A. (2023). Reinforcement learning for swarm robotics: An overview of applications, algorithms and simulators. *Cognitive Robotics*.

Chovancová, A., Fico, T., Chovanec, L., and Hubinsk, P. (2014). Mathematical modelling and parameter identification of quadrotor (a survey). *Procedia Engineering*, **96**, pp. 172–181.

Enwerem, C. and Baras, J. S. (2023a). Consensus-based leader-follower formation tracking for control-affine nonlinear multiagent systems. In *2023 9th International Conference on Control, Decision and Information Technologies (CoDIT)*, IEEE, pp. 1226–1231.

Enwerem, C. and Baras, J. S. (2023b). Consensus-based leader-follower formation tracking for control-affine nonlinear multiagent systems. In *2023 9th International Conference on Control, Decision and Information Technologies (CoDIT)*, IEEE, pp. 1226–1231.

Hehn, M. and D'Andrea, R. (2011). Quadrocopter trajectory generation and control. *IFAC proceedings Volumes*, **44** (1), pp. 1485–1491.

Ivanov, D., Zhdanov, A., and Sandler, I. (2024). Identification of dynamical systems with time-varying disturbances and fractional errors-in-variables. application example to a drone model. *Cybernetics and Physics*, **13** (1), pp. 49–56.

Kadhim, E. H. and Abdulsadda, A. T. (2022). Mini drone linear and nonlinear controller system design and analyzing. *Journal of Robotics and Control (JRC)*, **3** (2), pp. 212–218.

Kumar, S. and Dewan, L. (2020). Different control scheme for the quadcopter: a brief tour. In *2020 First IEEE International Conference on Measurement, Instrumentation, Control and Automation (ICMICA)*, IEEE, pp. 1–6.

Kumar, S. and Dewan, L. (2023a). Hybrid controller for soft landing of a quadcopter. *IETE Journal of Research*, pp. 1–14.

Kumar, S. and Dewan, L. (2023b). Quadcopter stabilization using hybrid controller under mass variation and disturbances. *Journal of Vibration and Control*, **29** (21-22), pp. 4857–4874.

Lee, D., Jin Kim, H., and Sastry, S. (2009). Feedback linearization vs. adaptive sliding mode control for a quadrotor helicopter. *International Journal of control, Automation and systems*, **7**, pp. 419–428.

Nguyen, L. V., Tran, H.-D., Johnson, T., and Gupta, V. (2023). Decentralized safe control for distributed cyber-physical systems using real-time reachability analysis. *IEEE Transactions on Control of Network Systems*, **10** (3), pp. 1234–1244.

Ribeiro, T. T., Conceiçao, A. G., Sa, I., and Corke, P. (2015). Nonlinear model predictive formation control for quadcopters. *IFAC-PapersOnLine*, **48** (19), pp. 39–44.

Rigatos, G. (2021). A nonlinear optimal control approach for the uav and suspended payload system. *Cybernetics and Physics*, **10** (1), pp. 27–39.

Saini, N. and Ohri, J. (2023). Load frequency control in three-area single unit power system considering nonlinearities effect. *Cybern. Phys., no*, **12** (1), pp. 60–69.

Sharma, A. and Handa, H. (2022). Synchronization and anti–synchronization of coupled lorenz chaotic systems. In *2022 International Conference on Electronics and Renewable Systems (ICEARS)*, IEEE, pp. 239–243.

Sharma, A., Vanjani, P., Paliwal, N., Basnayaka, C. M. W., Jayakody, D. N. K., Wang, H.-C., and Muthuchidambaranathan, P. (2020). Communication and networking technologies for uavs: A survey. *Journal of Network and Computer Applications*, **168**, pp. 102739.

Thanh, H. L. N. N. and Hong, S. K. (2018). Quadcopter robust adaptive second order sliding mode control based on pid sliding surface. *IEEE Access*, **6**, pp. 66850–66860.

Yagiz, N., Hacioglu, Y., and Taskin, Y. (2011). Sliding mode control of a vehicle with non-linearities.

Yanmaz, E., Yahyanejad, S., Rinner, B., Hellwagner, H., and Bettstetter, C. (2018). Drone networks: Communications, coordination, and sensing. *Ad Hoc Networks*, **68**, pp. 1–15.

Yao, H. and Liu, Z. (2010). The application of contraction theory in synchronization of coupled chen systems. *International Journal of Nonlinear Science*, **9** (1), pp. 72–77.

Zhang, C., Yang, Z., Zhuo, H., Liao, L., Yang, X., Zhu, T., and Li, G. (2023). A lightweight and drift-free fusion strategy for drone autonomous and safe navigation. *Drones*, **7** (1), pp. 34.